ADJOINT HARMONIC BALANCE METHOD FOR FORCED RESPONSE ANALYSIS IN TURBOMACHINERY

ANNA ENGELS-PUTZKA, CHRISTIAN FREY

German Aerospace Center (DLR), Institute of Propulsion Technology
Linder Höhe, 51147 Cologne, Germany
e-mail: Anna.Engels-Putzka@dlr.de, Christian.Frey@dlr.de

Key words: Aeroelasticity, Forced Response, Adjoint Methods, Harmonic Balance

Abstract. This paper describes the derivation and implementation of the discrete adjoint equations based on frequency domain methods (linear harmonics and harmonic balance) within a turbomachinery CFD code. Applications to model problems are presented which demonstrate the potential of the method for multidisciplinary turbomachinery problems, e.g. aeroelastics or aeroacoustics.

1 INTRODUCTION

Computational fluid dynamics (CFD) is increasingly used to improve the performance of turbomachinery components on the basis of numerical simulations. However, typical measures to increase the aerodynamic performance or to reduce the component weight imply a higher susceptibility to blade vibrations. Therefore, as the designs approach the aerodynamic optimum, the design problem becomes more and more multi-disciplinary. The application that the authors have in mind is a design optimisation where an aerodynamic objective (e.g. isentropic efficiency) and aeroelastic constraints (e.g. fatigue strength) are competing goals.

When going from the evaluation of a single design to CFD-based optimisation, it is important to compute also gradients of the objective functions and constraints with respect to design parameters. Since in typical applications the number of design parameters is much larger than the number of objectives, it is advantageous to use the adjoint method [1, 2]. While stationary adjoint methods are nowadays established also in the field of turbomachinery design (see e.g. [3, 4]), the use of instationary adjoint CFD is very limited due to its exceedingly high computational costs, see e.g. [5, 6, 7] and references therein.

The goal of this paper is to demonstrate how adjoint methods can be applied to frequency domain methods. These have been successfully employed for turbomachinery aeroelastic analysis, see [8] for an overview. In particular, the linear harmonic (LH) [9], the nonlinear harmonic (NLH) [10], and the harmonic balance (HB) [11] approaches are

widely used to simulate forced response and flutter. In the context of aeroelastic analysis, adjoint methods have been applied to LH methods [12, 13] as well as HB methods [14, 15, 16], and to the formulation of the HB equations for one harmonic in the time-domain [17]. In this paper, it is shown how to derive the discrete adjoint for the frequency domain methods implemented in the DLR flow solver TRACE [18, 19]. The methodology and solution techniques used for the discrete adjoint steady solver [20] are carried over to the LH and HB solvers [21, 22, 23].

2 THEORY

2.1 Frequency Domain Methods

We present here briefly the harmonic balance method as implemented in TRACE, for details we refer to [22, 23]. For simplicity we restrict the discussion to a single base frequency ω. The time-dependent flow solution $q(x, t)$ is approximated as a Fourier series where a finite number K of higher harmonics is taken into account:

$$q(x,t) = \mathrm{Re}\left[\sum_{k=0}^{K} \hat{q}_k(x) e^{ik\omega t}\right]. \tag{1}$$

Inserting this into the the time-dependent flow equation

$$\frac{d}{dt}q(x,t) + R(q) = 0, \tag{2}$$

where R is the discretised RANS residual, one obtains the following system of equations for the Fourier components $\hat{q}_k$:

$$ik\omega\hat{q}_k + \widehat{R(q)}_k = 0, \quad k = 0, \ldots, K. \tag{3}$$

Since R is nonlinear, the k-th harmonic of the residual, $\widehat{R(q)}_k$, may depend on all harmonics of q. Therefore, it is approximated using the Discrete Fourier Transform (DFT) for a set of sampling points $t_1, \ldots, t_n \in [0, 2\pi/\omega]$:

$$\widehat{R(q)}_k \approx \mathscr{F}(R(\mathscr{F}^{-1}(\hat{q})))|_k. \tag{4}$$

$\mathscr{F}^{-1}$ denotes the inverse transform, i.e. the reconstruction $\mathscr{F}^{-1}(\hat{q}) = (q(t_1), \ldots, q(t_n))^T$, where $q(t_j)$ is given by (1) for $t = t_j$. In the case of equidistant sampling points, i.e. $t_j = \frac{2\pi j}{\omega N}$, we obtain

$$q(x, t_j) = \mathrm{Re}\left[\sum_{k=0}^{K} e^{ik\frac{2\pi j}{N}} \hat{q}_k(x)\right], \quad j = 0, \ldots, N-1. \tag{5}$$

The corresponding Fourier coefficients are then given by

$$\hat{q}_0(x) = \frac{1}{N} \sum_{j=0}^{N-1} q(x, t_j) \tag{6}$$

$$\hat{q}_k(x) = \frac{2}{N} \sum_{j=0}^{N-1} e^{-ik\frac{2\pi j}{N}} q(x, t_j), \quad k = 1, \dots, K. \tag{7}$$

When the amplitudes of the harmonic perturbations ($|\hat{q}_k|$ for $k > 0$) are small, we can approximate the nonlinear Residual $R(q)$ by its linearisation about the time average, i.e.

$$R(q(t)) = R(\hat{q}_0) + \frac{\partial R}{\partial q}\Big|_{\hat{q}_0}(q(t) - \hat{q}_0). \tag{8}$$

Then the different harmonics decouple and we obtain the steady equation $R(\hat{q}_0) = 0$ and a linear equation for each $k > 0$ [21, 24]:

$$\left(ik\omega + \frac{\partial R}{\partial q}\Big|_{\hat{q}_0}\right)\hat{q}_k = 0. \tag{9}$$

2.2 Discrete Adjoint Approach

Similar to the stationary case (see e.g. [20]) we derive the discrete adjoint equations for the frequency domain methods. We assume that the objective functional I depends on a set of parameters α only through the Fourier coefficients of q, i.e.

$$\frac{dI}{d\alpha} = \frac{\partial I}{\partial \hat{q}} \frac{d\hat{q}}{d\alpha}. \tag{10}$$

For the purpose of this paper we assume that α is a parameter which influences only the values prescribed by an inhomogeneous (gust) boundary condition. Starting with the linearised equations , such a boundary condition yields an additional source term, so that (9) takes the form $A_k\hat{q}_k = S_{k,\alpha}$ [24]. From this we obtain immediately an equation for $\frac{d\hat{q}}{d\alpha}$, which can be used to eliminate this term from (10):

$$\frac{dI}{d\alpha} = \frac{\partial I}{\partial \hat{q}} A^{-1} \frac{\partial S_\alpha}{\partial \alpha} = \left((A^{-1})^* \left(\frac{\partial I}{\partial \hat{q}}\right)^*\right)^* \frac{\partial S_\alpha}{\partial \alpha} =: \hat{\psi}^* \frac{\partial S_\alpha}{\partial \alpha}, \tag{11}$$

where we have omitted the index k to simplify the notation. In the last step we have introduced the adjoint variables $\hat{\psi}$, which can be obtained by solving

$$A^*\hat{\psi} = \left(\frac{\partial I}{\partial \hat{q}}\right)^*. \tag{12}$$

For the adjoint harmonic balance method, we have to differentiate (3) with respect to α. Setting $R_{\mathrm{HB},k} := ik\omega\hat{q}_k + \widehat{R(q)}_k$, we get

$$
\begin{aligned}
0 &= \frac{dR_{\mathrm{HB},k}}{d\alpha} = \frac{\partial R_{\mathrm{HB},k}}{\partial \hat{q}}\frac{d\hat{q}}{d\alpha} + \frac{\partial R_{\mathrm{HB},k}}{\partial \alpha} \\
&= \sum_j \left(ik\omega\delta_{jk} + \frac{\partial \widehat{R(q)}_k}{\partial \hat{q}_j} \right)\frac{d\hat{q}_j}{d\alpha} + \frac{\partial R_{\mathrm{HB},k}}{\partial \alpha}.
\end{aligned}
\tag{13}
$$

The derivation of the adjoint equations is now analogous to the linear case, with $\frac{\partial S_\alpha}{\partial \alpha}$ replaced by $-\frac{\partial R_{\mathrm{HB},k}}{\partial \alpha}$. The explicit form is not discussed here, since it is only needed for the evaluation of sensitivities, which we do not consider in this article. To compute the system matrix A and its adjoint, we use the approximation (4) for the Fourier coefficients of the residual, and since $\mathscr{F}$ and $\mathscr{F}^{-1}$ are linear operations, we obtain

$$
D(\widehat{R(q)}) = \mathscr{F}\left(\mathrm{diag}\left(\left.\frac{\partial R}{\partial q}\right|_{q(t_j)} \right) \right)\mathscr{F}^{-1}
\tag{14}
$$

where $\mathrm{diag}(\ldots)$ denotes a block diagonal matrix with the corresponding entries on the diagonal. The submatrices are computed by reconstructing the flow solution at the sampling points t_j according to (5) and evaluating the residual Jacobian at each of these flow states.

To determine the adjoint of the matrix $D(\widehat{R(q)})$, we have to find the adjoints of $\mathscr{F}$ and $\mathscr{F}^{-1}$. The Fourier coefficients $\hat{q}$ are complex vectors, but the transformation $\mathscr{F}$ is not linear over the complex numbers. Therefore we consider all vectors as elements in real vector spaces and define the scalar product by

$$
\langle \hat{\psi}, \hat{q} \rangle = \mathrm{Re}\langle \hat{\psi}, \hat{q} \rangle_{\mathbb{C}}.
\tag{15}
$$

The resulting adjoint transformations are given by

$$
\psi(t_j) = (\mathscr{F}^*\hat{\psi})(t_j) = \frac{1}{N}\mathrm{Re}(\hat{\psi}_0) + \frac{2}{N}\mathrm{Re}\left[\sum_{k=1}^K e^{ik\frac{2\pi j}{N}}\hat{\psi}_k \right]
\tag{16}
$$

$$
\hat{\psi}_k = ((\mathscr{F}^{-1})^*\psi)_k = \sum_{j=1}^N e^{-ik\frac{2\pi j}{N}}\psi(t_j).
\tag{17}
$$

The complete adjoint system matrix is then

$$
A^* = \left(\mathscr{F}^{-1}\right)^*\left(\mathrm{diag}\left(\left.\frac{\partial R}{\partial q}\right|_{q(t_j)} \right) \right)^*\mathscr{F}^* - \mathrm{diag}(ik\omega).
\tag{18}
$$

3   IMPLEMENTATION

In TRACE, the steady discrete adjoint equations are solved by a preconditioned GMRes (Generalized Minimal Residual) algorithm with restarts. This has now been extended to treat several harmonics at the same time, either uncoupled (adjoint LH) or coupled (adjoint HB). The main difference for the coupled approach is that the multiplication by the system matrix is replaced by several operations according to (18). First, the adjoint solution vector is transformed into the time domain by an adjoint DFT. Then, for each sampling point, the corresponding matrix is applied, and the result is transformed back into the frequency domain. Finally, the frequency term (the original vector multiplied by $-ik\omega$) is added for each harmonic. For the computation of the matrices, the primal flow solution is reconstructed at the same sampling points as are used for the transformation of the solution vectors and the residual Jacobian is evaluated (numerically) at these flow states. For preconditioning, we use the Jacobian computed at the time-mean solution and only modify the diagonal by adding the frequency term corresponding to the current harmonic. The inverses of the modified diagonals are precomputed and stored for all harmonics. The preconditioner used in the following applications is SSOR with a relaxation factor of 0.7.

All boundary conditions are applied in the frequency domain, for each harmonic component separately. For this purpose, the stationary adjoint boundary conditions have been extended to treat complex vectors and the nonreflecting boundary conditions used at entries and exits (see [25]) now take into account the frequency, analogous to the linear solver.

Like the existing adjoint and linear solvers, the modified solver works on structured grids only and employs the constant eddy viscosity assumption. This means that possible dependencies of the eddy viscosity on the parameter α are not taken into account.

For this prototype implementation we consider only one objective functional, namely the entropy at the exit. More precisely, we consider the radial average of the circumferential Fourier coefficients for a given wave number.

4   APPLICATION

4.1   Numerical test case

As a simple numerical test case we use a segment of an annular duct with constant flow conditions. For the forward computation, an entropy wave is prescribed at the entry. The corresponding adjoint computation is done using the entropy functional (evaluated at the exit) with the same circumferential wave number. Since the underlying mean flow is constant, there is in this case no difference between linear harmonic and harmonic balance computations, therefore we present only results for the harmonic balance method. In Fig. 1 the density component of the harmonic balance solution for a plane wave propagating in axial direction, i.e. circumferential wave number zero, and the first component of the corresponding adjoint solution are shown. The adjoint solution represents the sensitivity

of the entropy functional with respect to sources in the flow field. The solutions are reconstructed from the first harmonic at four different points in time. As expected, we observe the same wave length and propagation speed in both cases.
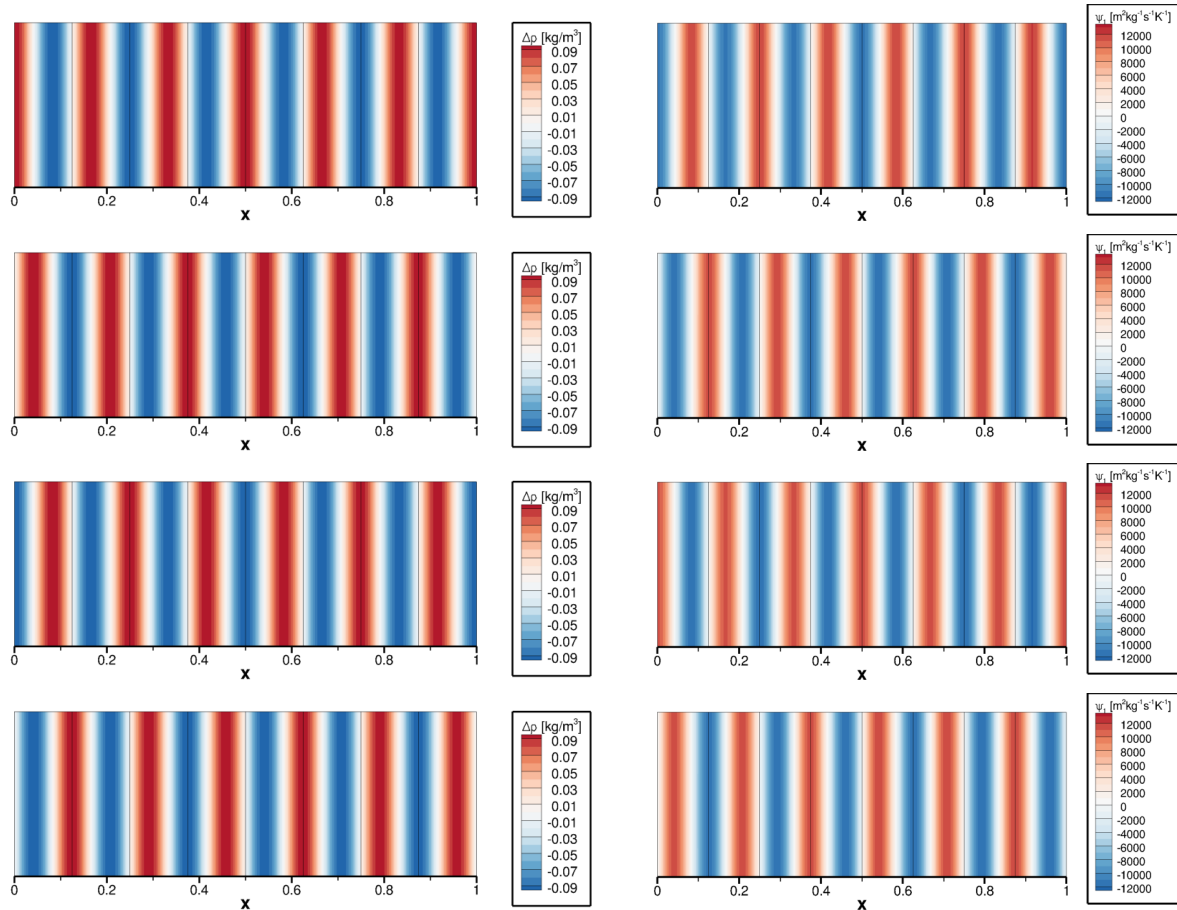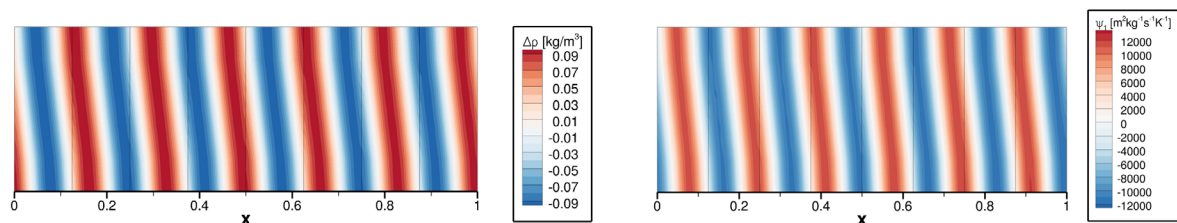

Figure 1: Reconstructed solutions (using the first harmonic) at four different times. Left: HB simulation of the propagation of an entropy wave. Right: Adjoint HB computation for the entropy functional.

In Fig. 2, the same results – but only for one point in time – are shown for a wave with a phase shift corresponding to a circumferential wave number of 16, where a similar relation between forward and adjoint solution can be observed.

4.2 Turbine rotor

As a model problem for turbomachinery applications we consider a configuration consisting of a single blade row, namely the rotor from a high pressure turbine stage. The flow conditions are subsonic with a maximum Mach number of about 0.78. The wake of the stator is extracted from a steady computation and the circumferential component with wave number $m = 70$, which corresponds to a phase shift (inter-blade phase an-

Figure 2: Reconstructed solutions (using the first harmonic) at $t = 0$. Left: HB simulation of the propagation of an entropy wave with circumferential wave number 16. Right: Adjoint HB computation for the entropy functional.

gle) of 60 degrees, is prescribed as gust boundary condition at the entry of the rotor. Computations with one and two higher harmonics are carried out. Figure 3 shows the entropy contours for the time-averaged solution and for the reconstructed solution using two higher harmonics. Although the inhomogeneous boundary condition is only used for the first harmonic, the coupling leads to a nonzero result in the second harmonic, but its magnitude is much smaller than that of the first (see Fig. 4). The effect of the coupling can also be seen in a comparison of a linear harmonic and a harmonic balance computation, each with one higher harmonic (Fig. 5).
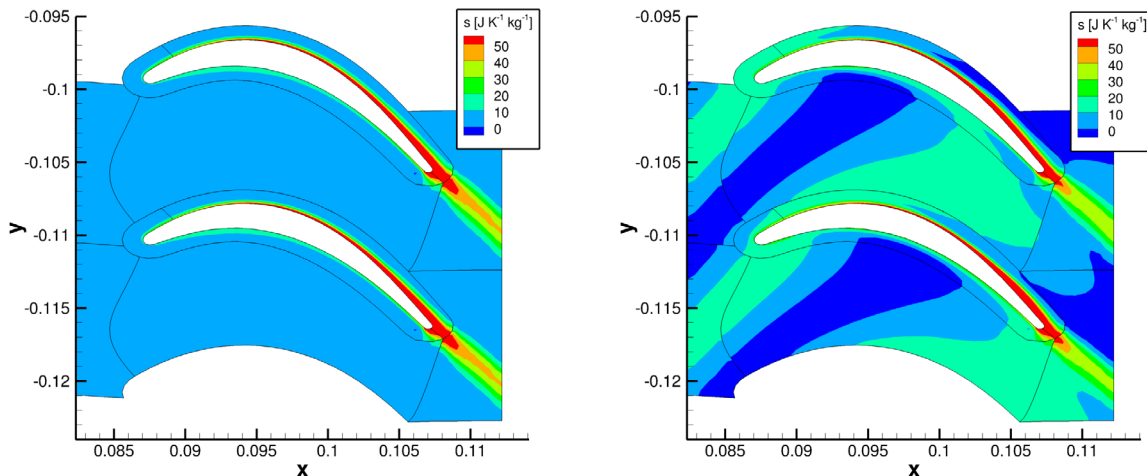

Figure 3: Entropy contours of the time averaged solution (left) and reconstructed instationary solution using two higher harmonics (right).

Similarly, in Fig. 6 we compare the results from the adjoint LH and adjoint HB methods for a computation including the zeroth and first harmonic. Some differences can be observed, although the overall structure of the solution is similar. In addition, we also carried out an adjoint HB computation with the second harmonic added, but only for the

651
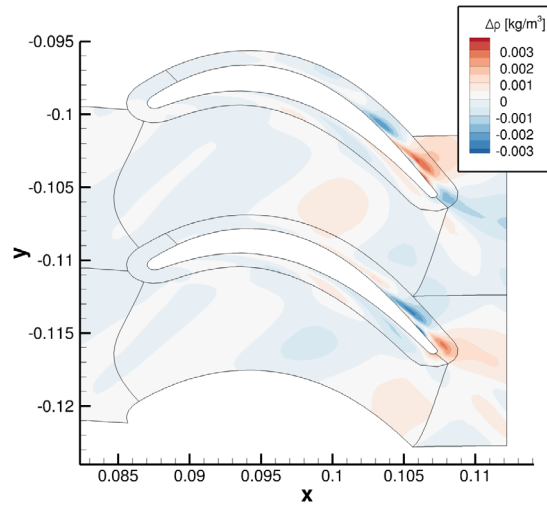
Figure 4: Second harmonic of density, reconstructed at $t = 0$, from a harmonic balance computation using two higher harmonics.
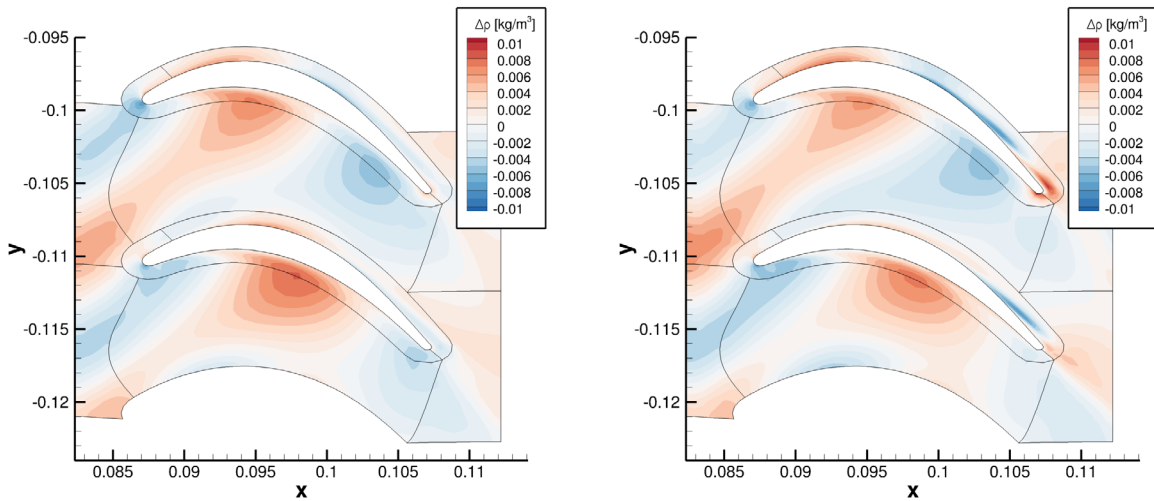

Figure 5: First harmonic of density, reconstructed at $t = 0$, from a linear harmonic (left) and a harmonic balance (right) computation including the zeroth and first harmonics.

first harmonic a non-zero right hand side is prescribed. Figure 7 shows that, as in the forward computation nonlinear effects lead to a non-negligible amplitude in the second harmonic of the adjoint solution, and also the solution for the first harmonic changes due to the coupling.
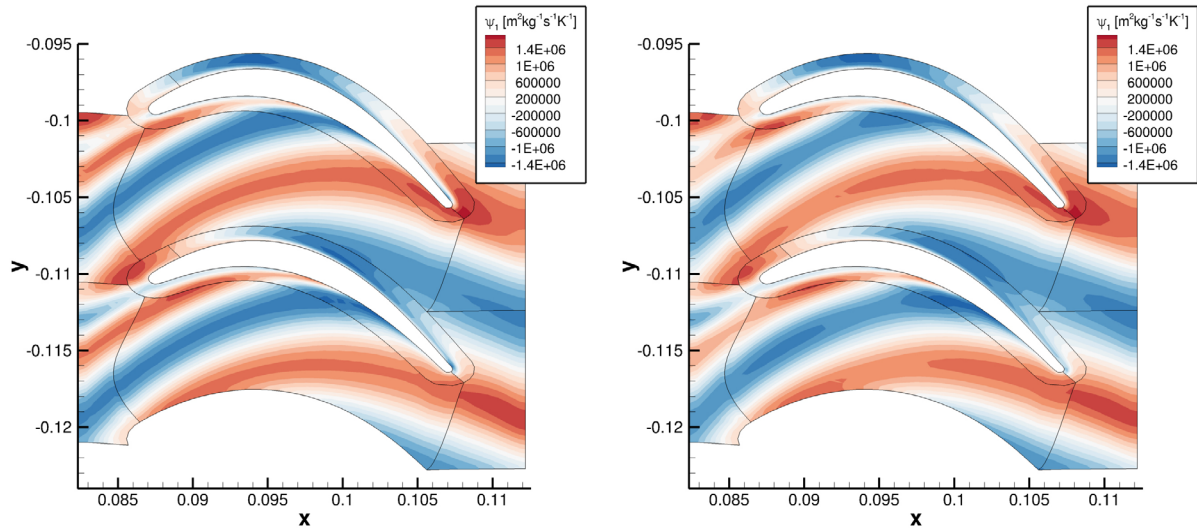
Figure 6: Density component of the adjoint solution for the entropy functional in the time domain (at $t = 0$) reconstructed using the first harmonic for linear harmonic (left) and harmonic balance (right) method.
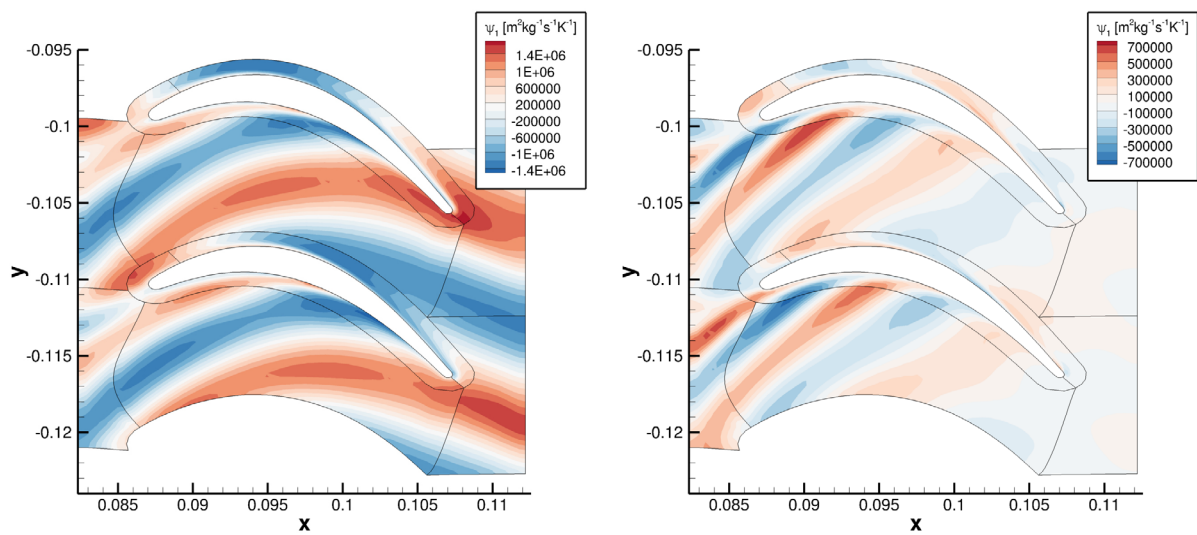
Figure 7: Density component of the first (left) and second (right) harmonic of the adjoint solution in the time domain (at $t = 0$) for the entropy functional from an adjoint HB computation using two higher harmonics.

In Fig. 8, a comparison of the convergence histories for different setups is shown. The convergence of the adjoint linear harmonic computation is similar to the steady adjoint and forward linear harmonic computations, if the linear system is solved over the complex numbers. If it is treated as a real system within the GMRes algorithm, the convergence becomes somewhat slower. The convergence behaviour of the adjoint harmonic balance computations depends strongly on the number of harmonics. If only one harmonic (besides the zeroth) is considered, the convergence is still similar to that of the adjoint linear harmonic computation using GMRes in real mode. If two higher harmonics are included, significantly more iterations are needed. It has to be investigated if the convergence can be improved by different GMRes settings (e.g. restart interval or preconditioner) or if other solution techniques, e.g. pseudo-time marching, are more suitable for this kind of problems.
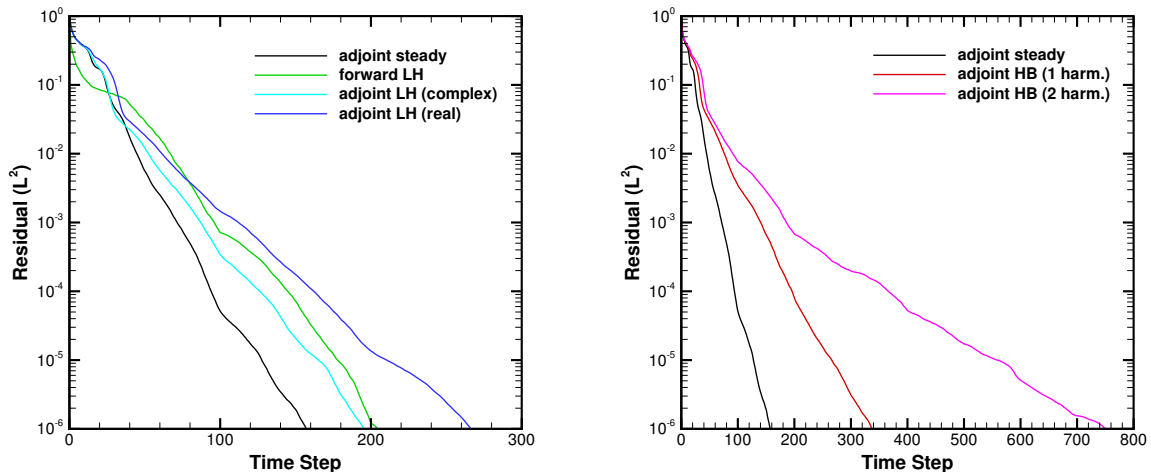
Figure 8: Convergence history for linear harmonic, adjoint linear harmonic and adjoint harmonic balance computations compared with a steady adjoint computation. All computations have been carried out using a restart interval of 100.

5 CONCLUSION

We have presented the derivation and implementation of adjoint frequency domain methods based on existing implementations of the linear harmonic and harmonic balance techniques. The functionality has been demonstrated using two model problems. The application to a turbine rotor shows the potential of the method for turbomachinery applications. Although the adjoint harmonic balance computations need significantly more computational time than the stationary adjoint, there is still a large speedup expected with respect to instationary adjoint methods in the time domain.

However, it has to be investigated if the current approach is also suitable for more complex problems or if different solution strategies are needed. Further topics for future work include the implementation of functionals which are relevant for aeroelastic analysis (e.g. modal work), the evaluation of sensitivities with respect to design parameters, the treatment of different boundary conditions and preconditioners, and the extension to several blade rows.

REFERENCES

[1] Jameson, A. Aerodynamic design via control theory. *J. Sci. Comput.* (1988) **3**(3):233–260.

[2] Giles, M.B. and Pierce, N.A. An introduction to the adjoint approach to design. *Flow Turbul. Combust.* (2000) **65**:393–415.

[3] Wang, D.X. and He, L. Adjoint aerodynamic design optimization for blades in multistage turbomachines—part I: Methodology and verification. *J. Turbomach.* (2010) **132**(2):021011.

[4] Wang, D.X., He, L. and Li, Y.S., Wells, R.G. Adjoint aerodynamic design optimization for blades in multistage turbomachines—part II: Validation and application. *J. Turbomach.* (2010)**132**(2):021012.

[5] Nadarajah, S.K. and Jameson, A. Optimum shape design for unsteady flows with time-accurate continuous and discrete adjoint methods. *AIAA J.* (2007) **45**(7):1478–1491.

[6] Nielsen, E.J. and Diskin, B. Discrete Adjoint-Based Design for Unsteady Turbulent Flows on Dynamic Overset Unstructured Grids. *AIAA J.* **51**(6), 1355–1373 (2013).

[7] Ntanakas, G. and Meyer, M. Towards unsteady adjoint analysis for turbomachinery applications. Proceedings of the 6th. European Conference on Computational Fluid Dynamics - ECFD VI, pp. 5071–5081 (2014).

[8] He, L. Fourier methods for turbomachinery applications. *Prog. Aerosp. Sci.* (2010) **46**(8):329–341.

[9] Hall, K.C. and Crawley, E.F. Calculation of unsteady flows in turbomachinery using the linearized Euler equations. *AIAA J.* (1989) **27**(6):777–787.

[10] He, L. and Ning, W. Efficient approach for analysis of unsteady viscous flows in turbomachines. *AIAA J.* (1998) **36**(11):2005–2012.

[11] Hall, K.C., Thomas, J.P. and Clark, W.S. Computation of unsteady nonlinear flows in cascades using a harmonic balance technique. *AIAA J.* (2002) **40**(5):879–886.

[12] Duta, M.C., Giles, M.B. and Campobasso, M.S. The harmonic adjoint approach to unsteady turbomachinery design. *Int. J. Numer. Methods Fluids* (2002) **40**(3-4):323–332.

[13] Duta, M., Campobasso, M., Giles, M. and Lapworth, L. Adjoint harmonic sensitivities for forced response minimization. *J. Eng. Gas Turbines Power* (2006) **128**(1):183–189.

[14] Thomas, J., Hall, K. and Dowell, E. Discrete adjoint approach for modeling unsteady aerodynamic design sensitivities. *AIAA J.* (2005) **43**(9):1931–1936.

[15] Nadarajah, S.K., McMullen, M.S. and Jameson, A. Aerodynamic shape optimization for unsteady three-dimensional flows. *Int. J. Comput. Fluid Dyn.* (2006) **20**(8):533–548.

[16] Nadarajah, S.K. and Jameson, A. Optimum shape design for unsteady three-dimensional viscous flows using a nonlinear frequency-domain method. *J. Aircraft* (2007) **44**(5):1513–1527.

[17] He, L. and Wang, D.X. Concurrent Blade Aerodynamic-Aero-elastic Design Optimization Using Adjoint Method. *J. Turbomach.* (2011) **133**(1):011021.

[18] Nürnberger, D., Eulitz, F., Schmitt, S. and Zachcial, A. Recent progress in the numerical simulation of unsteady viscous multistage turbomachinery flow. ISABE 2001-1081 (2001).

[19] Becker, K., Heitkamp, K. and Kügeler, E. Recent progress in a hybrid-grid CFD solver for turbomachinery flows. Proceedings Fifth European Conference on Computational Fluid Dynamics ECCOMAS CFD 2010 (2010).

[20] Frey, C., Nürnberger, D. and Kersken, H.P. The discrete adjoint of a turbomachinery RANS solver. Proceedings of ASME-GT2009 (2009).

[21] Kersken, H.P., Frey, C., Voigt, C. and Ashcroft, G. Time-Linearized and Time-Accurate 3D RANS Methods for Aeroelastic Analysis in Turbomachinery. *J. Turbomach.* (2012) **134**(5):051024.

[22] Frey, C., Ashcroft, G., Kersken, H.P. and Voigt, C. A harmonic balance technique for multistage turbomachinery applications. Proceedings of ASME Turbo Expo 2014 (2014).

[23] Ashcroft, G., Frey, C. and Kersken, H.P. On the development of a harmonic balance method for aeroelastic analysis. 6th European Conference on Computational Fluid Dynamics (ECFD VI) (2014).

[24] Frey, C., Ashcroft, G., Kersken, H.P. and Weckmüller, C. Advanced numerical methods for the prediction of tonal noise in turbomachinery — Part II: Time-linearized methods. *J. Turbomach.* (2013) **136**(2):021002.

[25] Frey, C., Engels-Putzka, A. and Kügeler, E. Adjoint boundary conditions for turbomachinery flows. ECCOMAS 2012 - European Congress on Computational Methods in Applied Sciences and Engineering, e-Book Full Papers (2012).